Journal of Innovation and Development
ISSN: 2958-4752 | Vol. 11, No. 1, 2025

Angle Control of Independent Drive Differential Steering Wheelset

Jiaqi Zhang[1,*], Cunsheng Zhang[1], Gaofei Qu[2]

[1]School of Mechanical and Power Engineering, Henan Polytechnic University, Jiaozuo 454003, China
[2]Jiaozuo Creation Heavy Industry Co., Ltd, Jiaozuo, China
[*] Corresponding author: Jiaqi Zhang (Email: zjqlc1014@163.com)

Abstract: This study investigates the relative angle control between a single wheelset and the chassis, taking into account the independent rotation of each wheelset in the four-wheel steering chassis with four differential wheelsets. To ensure coordinated and stable chassis motion while adjusting the wheelset angle, it is necessary to account for the impact of wheelset speed on the overall dynamics of the chassis. This research aims to introduce an uncomplicated yet potent control technique to ad-dress the identified problem. Initially, the dynamic equation governing wheel motion was formulated. Subsequently, ahierarchical control system integrating fuzzy PID and fuzzy-fuzzy PID elements was developed to modulate the wheelset angle, thereby ensuring its stable regulation along with the velocity. Simulations were conducted on a compact chassis model using the integrated MATLAB/Simulink and ADAMS simulation environment. These tests confirmed that the hierarchical control system adeptly controlled both the angular positioning and the linear velocity of the wheelset, meeting the locomotive requirements of the chassis.

Keywords: Cascade control; Wheelset angle control; Proportional integral derivative; Fuzzy.

1. Introduction

The all-wheel steering chassis is an innovative design, characterized by a small turning radius, flexible steering, and enhanced maneuverability. Advances in all-wheel steering and intelligent control technologies have been implemented to enhance chassis dynamic performance [1], playing a crucial role in military, industrial, transportation, and production sectors.

Researchers across various disciplines have made significant contributions to the control of all wheel steering chassis. Notably, Professor Jumming Wan's team at Ohio State University in the United States has developed a fully controlled four-wheel independent electric vehicle (GEV), primarily for integrated control of vehicle dynamics, and parameter estimation [6]. Wang Jie's team developed an innovative technology that combines differential drive with torque distribution control. This advancement significantly alleviates the steering torque required and preserves the tactile feedback during high-speed maneuvers [7]. Ni Jun et al. investigated layered chassis yaw dynamics control (CYDC) and tire force management for unmanned ground vehicles (UGVs) in remote control mode (RCM), and pro-posed a layered CYDC scheme that enhances vehicle per-formance [8]. Kuslit et al. presented a new concept of differ-ential steer by wire, which matches the effectiveness of traditional steering systems [9].

Classic control methods such as PID control and trajectory control necessitate complex and accurate modeling[10]. In contrast, intelligent control techniques utilizing fuzzy algorithms, neural network algorithms, and synovial control algorithms are simpler and more efficient, and can handle nonlinear problems in chassis motion. Nguyen et al. pro-posed a fuzzy steering system capable of accommodating large variations in vehicle speed [14]. Furthermore, Thanok et al. utilized particle swarm optimization (PSO) to fine-tune both the sliding surface and the controller gains within a sliding mode controller (SMC). This optimization significantly improved the longitudinal control capabilities of the vehicle [15].

The control techniques described predominantly cater to chassis with intricate steering configurations, aiming to bolster the steering system's stability and the overall safety of the drive mechanism. In contrast, a chassis that employs an eight-drive, four-differential wheelset with all-wheel steering presents a less complex steering architecture. The structur-al model of this chassis is illustrated in Figure 1. Its various motion modes depend on the coordinated changes of the wheel speeds of the eight individually driven wheels in the four wheelsets. Notably, there are no rigid constraint elements such as differentials or friction locks configured in the chassis wheelsets. Traditional control methods for the steering angle management in chassis wheelset often necessi-tate the development of complex control systems, making it challenging to achieve satisfactory results.

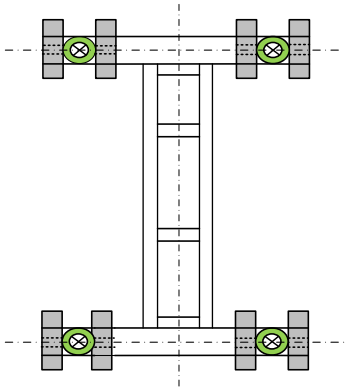

Figure 1. Floor plan model of the chassis

To attain coordinated and stable motion of the chassis, this paper proposes a fuzzy PID-fuzzy-fuzzy PID wheelset turn angle cascade control system for wheelset turn angles, tailored to the motion characteristics of a single wheelset. The feasibility of this control system was validated through joint simulation of the chassis using MATLAB/Simulink ADAMS

platform. This article primarily contributes the following: a designed fuzzy PID-fuzzy-fuzzy PID wheelset angle control system, which simultaneously considers the control of the relative angle between the wheel and chassis as well as the translational speed of the wheel, saves control costs, and improves the overall stability of the chassis motion.

2. Wheelset Modeling

This investigation focuses on the longitudinal, lateral, and yaw movements of the wheelset but does not con-sider the impact of tire deformation. The independent, adjustable driving torque of each wheel within the wheel-set directly affects their longitudinal forces. Variations in these forces across the left and right wheels lead to wheelset rotation, and alterations in the total longitudinal forces influence the wheelset's translational velocity. Figure 2 depicts the schematic of the wheelset's structural model.

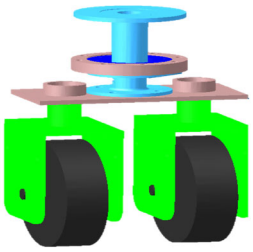

Figure 2. Schematic diagram of the structural model of the wheelset

In order to explore the control strategy for wheelset motion, a theoretical model of the wheel must be established. Figure 3 illustrates the force diagram for the wheel. The wheel's rotational angular velocity is denoted by ω_m, and its driving torque is denoted by T_e , along with the total weight and load on the wheel are represented as G. The wheel's moment of inertia is indicated by J_m, while M_f denotes the resistance torque exerted on the wheel. B signifies the viscous friction damping coefficient, a represents the wheel's diameter, and F_x refers to the longitudinal force exerted by the tire.

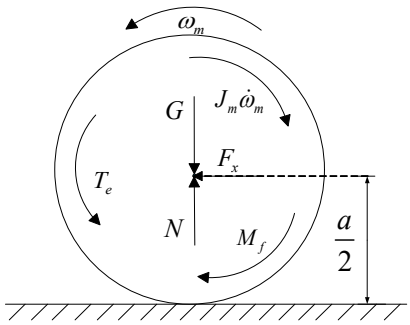

Figure 3. Force diagram for the wheel

From the force diagram in Figure 3, it can be seen that the relationship between the longitudinal force of the wheel and the rotational angular velocity of the wheels is:

$$F_x = \frac{2}{a}(T_e - B\omega_m - J_m\dot{\omega}_m - M_f) \tag{1}$$

According to the basic principles of dynamics, further obtain the dynamic equation of the wheelset (υ is the translational velocity of the wheelset, θ is the relative angle of rotation between the wheelset and the chassis, ω' is the lateral angular velocity of the chassis, and b is the center distance between the left and right wheels in the wheelset , J is the moment of inertia of the wheelset, m is the mass of the wheelset, T_{e_1} is the driving torque of the left wheel, T_{e_2} is the driving torque of the right wheel, M_{f_1} is the rotational resistance torque experienced by the left wheel , M_{f_2} is the rotational resistance torque experienced by the right wheel ,and F_τ is the longitudinal force exerted by the chassis on the wheelset at the steering knuckle):

$$\begin{bmatrix}\ddot{\theta}\\ \dot{\upsilon}\end{bmatrix} = \begin{bmatrix}\frac{-4b^2B}{a^2J+4b^2J_m} & 0\\ 0 & \frac{-4B}{a^2m+4J_m}\end{bmatrix}\begin{bmatrix}\dot{\theta}\\ \upsilon\end{bmatrix} + \begin{bmatrix}\frac{-2ab}{a^2J+4b^2J_m} & \frac{2ab}{a^2J+4b^2J_m}\\ \frac{2a}{a^2m+4J_m} & \frac{2a}{a^2m+4J_m}\end{bmatrix}\begin{bmatrix}T_{e_1}\\ T_{e_2}\end{bmatrix} + \begin{bmatrix}\frac{2ab(M_{f_1}-M_{f_2})-4b^2B\omega'}{a^2J+4b^2J_m}\\ \frac{-4ab(M_{f_1}+M_{f_2})-4a^2F_\tau}{8bJ_m+2a^2bm}\end{bmatrix} \tag{2}$$

The above equation shows that only the driving torques T_{e_1} and T_{e_2} of the left and right wheels in the wheelset are controllable. Consequently, speed control of the left and right wheels can be achieved by adjusting these driving torques, thereby enabling control over both the relative angle between the wheelset and the chassis and the overall speed of the wheelset.

3. Design of Wheelset Angle Control System

3.1. Analysis of Control Problems

The stability and coordination of the chassis depend critically on the velocity of each wheelset and their angular relationship with the chassis. Consequently, this investigation underscores the critical need for consistent, real-time regulation of both the wheelset's translational velocity and its angular orientation relative to the chassis. The designed control system should have good adaptability to facilitate practical engineering applications.

3.2. Architecture Design of Wheelset Angle Control System

The fuzzy logic controller is distinguished by its uncomplicated design and minimal cost of implementation [16]. It operates effectively without needing a precise mathematical representation of the system, thus ensuring consistent performance amidst dynamic shifts in control parameters and environmental condition [17]. This paper proposes a fuzzy PID fuzzy PID cascade control system for the differential wheelset. The structural model diagram is shown in Figure 4, where θ^* is the target angle between the

wheelset and the chassis, e is the angle error, υ is the target speed of the wheelset, y_1 and y_2 are the target speeds of the left and right wheels output by the fuzzy controller, E_1 and E_2 are the speed errors of the left and right wheels, T_{e_1} and

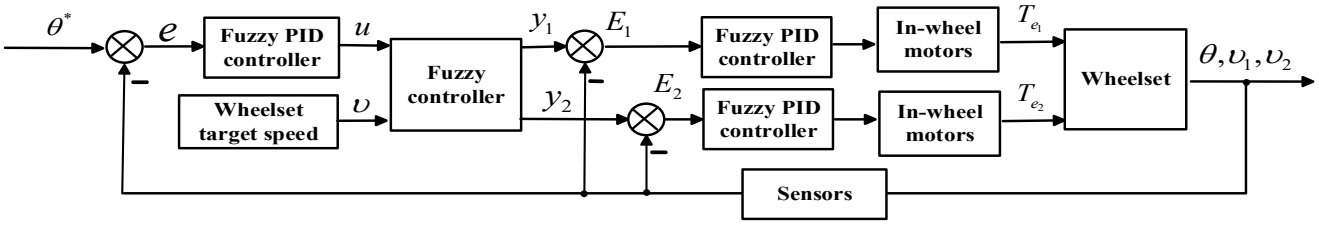

Figure 4. Structure diagram for the corner controller

T_{e_2} are the driving torque output by the hub motors of the left and right wheels, and θ, υ_1, and υ_2 are the actual angles between the wheelset and the chassis and the actual speeds of the left and right wheels, respectively.

The target relative angle θ^* between the wheelset and the chassis serves as the control input, and after processing through the fuzzy PID controller, outputs u. u and the expected speed of the wheelset as inputs to the fuzzy controller. The fuzzy controller transmits the anticipated speeds y_1 and y_2 for the left and right wheels of the wheelset to the wheel hub motor, utilizing a fuzzy PID controller to manage the motor's velocity. The hub motors generate driving torque to adjust the speed of the left and right wheels. The actual turning angle θ resulting from the speed difference between the wheels is used as feedback for the system, forming a closed-loop control system that manages the wheelset turning angle. The average of the left and right wheel speeds in the wheelset determines the translational speed of the wheelset. Among them, the Mamdani minimum operation algorithm is employed for fuzzy reasoning, and the centroid method is utilized for defuzzification.

3.3. Design of Fuzzy PID Controller

The fuzzy PID controller integrates a fuzzy control unit that dynamically fine-tunes the principal parameters of the PID system in real-time for enhanced speed and stability in control processes. Figure 5 depicts the architectural configuration of the fuzzy PID controller. The inputs to the fuzzy module, namely the error E and the rate of change of error E_c, along with the output variables ΔK_p, ΔK_i, and ΔK_d, are classified using seven fuzzy linguistic terms: negative big (NB), negative medium (NM), negative small (NS), zero (ZO), positive small (PS), positive medium (PM), and positive big (PB).

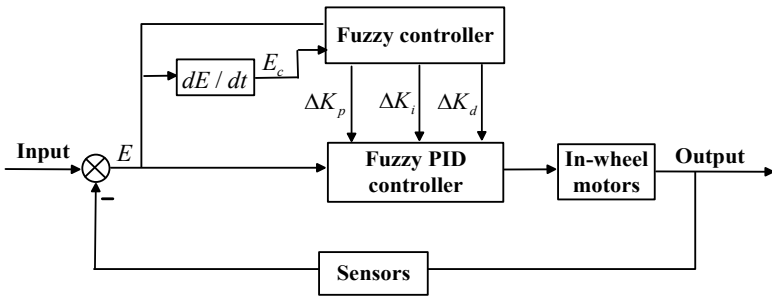

Figure 5. Structure Model for Fuzzy PID Controller

3.4. Design of Fuzzy Controller

To manage the wheel speed distribution for the left and right wheels of the differential wheelset, this study designs a dual input dual output fuzzy controller. The structural model diagram is shown in Figure 6. The output u from the upper level fuzzy PID and the target speed υ of the wheel set are used as inputs to the fuzzy controller, and the target speeds y_1 and y_2 of the left and right wheels output by the fuzzy controller are used as inputs to the lower level fuzzy PID. The actual domain of fuzzy input variable u is $\{-90 \sim 90\}$, and the fuzzy domain is set to $\{-4 \sim 4\}$. The corresponding fuzzy sets are di-vided into 9,namely (NB), (NM), (NS), negative zero (NZ), (ZO), positive zero (PZ), (PS), (PM), and (PB). The actual domain of the expected speed of υ for the wheelset is $\{-1 \sim 1\}$, and the fuzzy domain is set to $\{-4 \sim 4\}$. The corresponding fuzzy sets are divided into 8, namely (NB), (NM), (NS), (NZ), (PZ), (PS), (PM) and (PB) .The actual domain of the two wheel output speeds y_1 and y_2 is $\{-2 \sim 2\}$, and the fuzzy domain is taken as $\{-4 \sim 4\}$. The corresponding fuzzy sets are divided into 9, namely negative fast (NF), negative slower than fast (NRF), negative slow (NW), negative slower than slow (NRW), zero (ZO), positive slower than slow (PRW), positive slow (PW), positive slower than fast (PRF), and positive fast (PF). The membership functions of u, υ, y_1, and y_2 are shown in Figure 7.

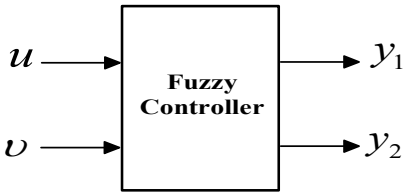

Figure 6. Structure Model for Fuzzy Controller

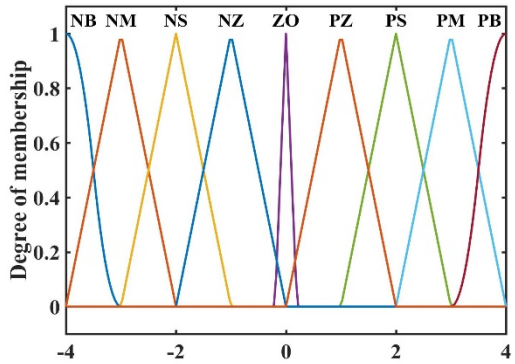

(a) Membership curve for u

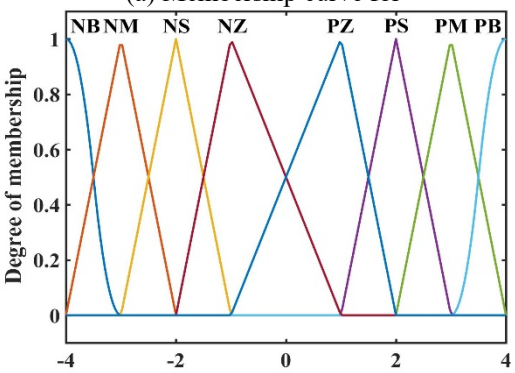

(b) Membership curve for υ

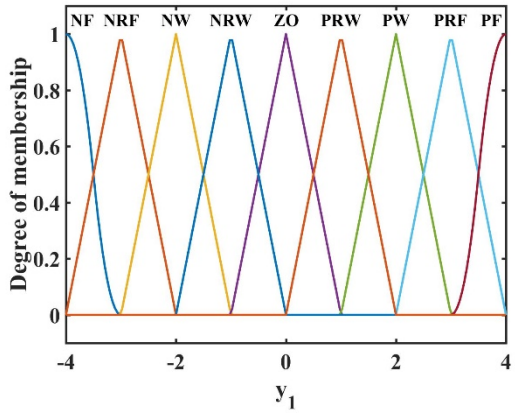

(c) Membership curve for y_1

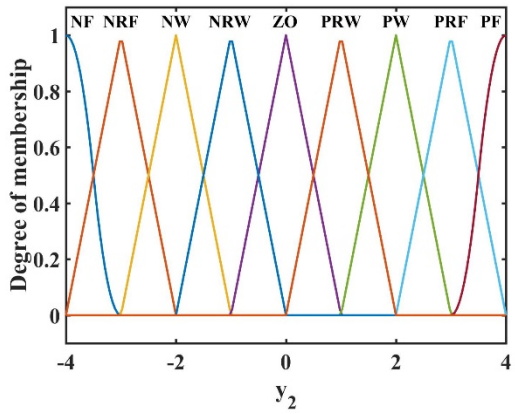

(d) Membership curve for y_2

Figure 7. Membership curve for input and output

The formulation of fuzzy rules is central to implementing fuzzy control. In order to achieve effective and stable cornering control, the following principles must be adhered to:

(1) A substantial angular error in the turning process necessitates implementing a significant velocity differential between the left and right wheels.

(2) With minimal deviation in the turning angle, it becomes imperative to diminish the speed disparity between the left and

right wheels to avert significant overshoot.

(3) When the steering angle error approaches zero, the wheel speeds of the left and right wheels should be equal, maintaining the wheelset's steering angle.

(4) When the chassis is moving rapidly, abrupt large-angle adjustments are prohibited.

(5) When the chassis speed is moderate, some angle adjustment is permitted.

(6) When the chassis speed is low, larger angle adjustments can be made in a short time frame.

(7) The velocities of the left and right wheels within the wheelset are expected to align closely with the predetermined speed designated for the wheelset.

The formulation of the above rules takes into account the motion state of the chassis, by reasonably allocating the speed of the left and right wheels in the wheelset, stable adjustment of the turning angle of each wheelset and stable control of the translational speed can be achieved thus improving the stability of the chassis during the turning angle adjustment process. Based on these rules, fuzzy rule tables have been established, as shown in Tables 1 and 2.

Table 1. Fuzzy rules for y_1

y_1		u								
		NB	NM	NS	NZ	ZO	PZ	PS	PM	PB
υ	NB	NRW	NRW	NRW	NW	NRF	NRF	NRF	NRF	NF
	NM	ZO	NRW	NRW	NW	NW	NRF	NRF	NRF	NF
	NS	ZO	NRW	NRW	NRW	NW	NW	NW	NRF	NRF
	NZ	ZO	ZO	ZO	ZO	NRW	NW	NW	NW	NW
	PZ	PW	PW	PW	PW	PRW	ZO	ZO	ZO	ZO
	PS	PRF	PRF	PW	PW	PW	PRW	PRW	PRW	ZO
	PM	PF	PRF	PRF	PRF	PW	PW	PRW	PRW	ZO
	PB	PF	PRF	PRF	PRF	PRF	PW	PRW	PRW	PRW

Table 2. Fuzzy rules for y_2

y_2		u								
		NB	NM	NS	NZ	ZO	PZ	PS	PM	PB
υ	NB	NF	NRF	NRF	NRF	NRF	NW	NRW	NRW	NRW
	NM	NF	NRF	NRF	NRF	NW	NW	NRW	NRW	NRW
	NS	NRF	NRF	NW	NW	NW	NRW	NRW	NRW	ZO
	NZ	NW	NW	NW	NW	NRW	ZO	ZO	ZO	ZO
	PZ	ZO	ZO	ZO	ZO	PRW	PW	PW	PW	PW
	PS	ZO	PRW	PRW	PRW	PW	PW	PW	PRF	PRF
	PM	ZO	PRW	PRW	PW	PW	PRF	PRF	PRF	PF
	PB	PRW	PRW	PRW	PW	PRF	PRF	PRF	PRF	PF

Figure 8 illustrates the graphical depiction of the relationship between inputs and outputs managed by the fuzzy controller.

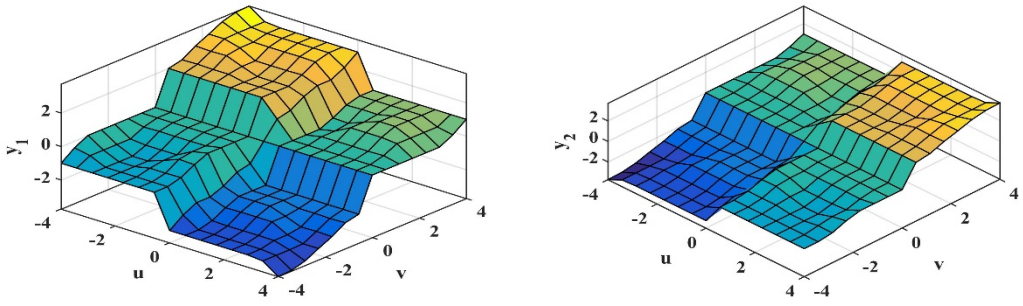

(a)Fuzzy rule surface for u , υ and y_1 (b) Fuzzy rule surface for u , υ and y_2

Figure 8. Fuzzy Rule Surface Diagram

The designed wheelset motion control system effectively manages the steering angle and wheel set translational speed of both the wheelset and chassis, featuring a straightforward structure, low cost, and ease of application.

4. Simulation and Analysis

To ascertain the viability of the wheelset angle control approach, a collaborative simulation involving the chassis was executed utilizing MATLAB/Simulink alongside ADAMS. The key parameters employed in the simulation are detailed in Table 3.

This simulation includes a human-computer interaction module, steering angle distribution system, wheelset steering angle controller, wheel speed distribution system, wheel

speed controller, detection module, signal processing module, and chassis model. Figure 9 displays the ADAMS model for the chassis. Following the construction of this model, definitions for the state variables were established. The input variables being the driving torque of eight wheels, and the output variables comprising the chassis motion speed, the rotation angle of four wheelsets, and the speed of eight wheels.

Table 3. Main parameters of joint simulation

Parameter	Description	value
m	Chassis quality	100kg
L	Chassis wheelbase	1150mm
W	Distance between the left and right wheelsets of the chassis	500mm
b	The center distance between the left and right wheels of the wheelset	156mm
m_q	Wheel set quality	4kg
B	Viscous friction damping coefficient	0.07N·m·s/rad
a	Wheel diameter	200mm
U	Rated voltage of motor	24V
I	Rated current of motor	12A
T	Rated torque of motor	0.72N·m
n	Rated speed of motor	3000rpm

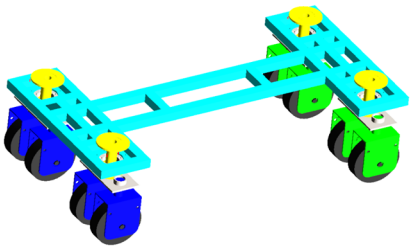

Figure 9. ADAMS model of the chassis

To assess the effectiveness of the control strategy, a comprehensive and continuous simulation was performed, mainly including: starting, accelerating, driving straight, turning, and obstacle crossing. During the maneuvering phase, the chassis steering system assigns designated steering angles of -20° and -28° to the left and right front wheel pairs, respectively, and 20° and 28° to the left and right rear wheel pairs. Concurrently, the orientation of the ladder obstacle relative to the chassis's front axle is established at a 20-degree angle. The simulation time is configured for 40 seconds with a step size of 0.005 seconds.

The chassis joint simulation results are illustrated in Figure 10. Control the chassis to accelerate from a standstill to 0.5m/s within 2 seconds, followed by uniform linear motion; At 8s, the chassis begins to decelerate to 0.2m/s in preparation for a turn; The turning action starts at 11 seconds, with all wheelset angles adjusted within 1 second; At 22.2s, the chassis transitions from turning to straight mode; At 29.5s, the left front wheel of the chassis contacts the left and right wheels of the vehicle in succession, followed by the left rear wheel at 35.7 seconds, successfully completing the obstacle crossing. The trajectory of the chassis center of mass is shown in Figure 11.

The simulation outcomes demonstrate that the chassis's motion path aligns precisely with the anticipated standards, showcasing a trajectory that is both consistent and smooth. During the straight driving process, the wheel speeds of each wheel remain consistent, the driving torque output is stable, and there is no significant change in the relative angle between each wheel and the chassis. During the turning process, the chassis speed fluctuates slightly within a controllable range, and the speed of.

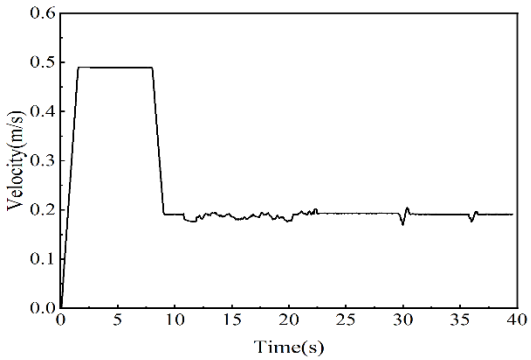

(a) The speed of the chassis

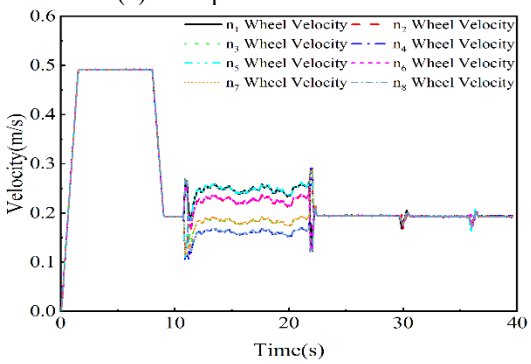

(b) The speed of eight wheels

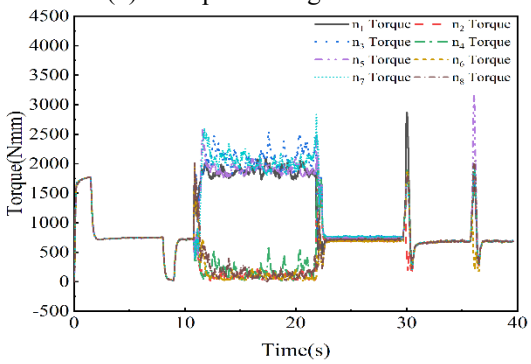

(c) The drive torque of eight wheels

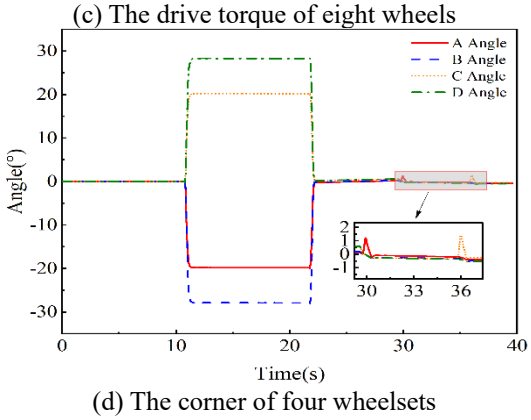

(d) The corner of four wheelsets

Figure 10. Chassis driving simulation result diagram

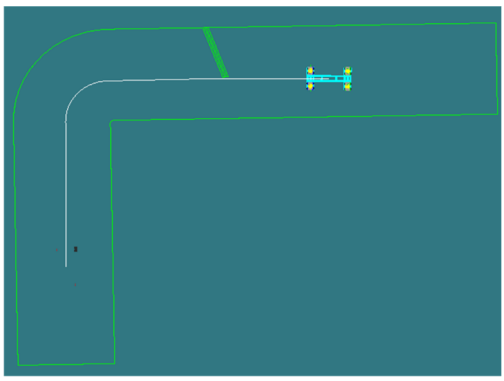

Figure 11. Trajectory of the chassis centroid

the left and right wheels of each wheelset changes in coordination, with stable adjustment of the wheelset angle. In scenarios involving a constant turning radius, the velocity of the chassis's left wheelset exceeds that of the right, necessitating a greater torque output from the left to effectively overcome the inherent rotational resistance torque experienced by the wheelsets. During the process of traversing obstacles, the relative rotational angles between the left front and left rear wheels deviated by approximately 2 degrees. This deviation prompted rapid adjustments in the velocities of the wheels within the specific wheelset. These adjustments continued until the rotation angles of the wheelset closely aligned with the anticipated values. Upon achieving this alignment, the differential in wheel speeds between the left and right sides was eliminated, leading to a cessation of adjustments. Consequently, the chassis resumed its progression in a stable and controlled manner.

5. Conclusion

(1) This article designs a fuzzy PID fuzzy PID cascade control system for the independent drive differential steering wheelset angle, which can effectively control the relative angle between the chassis and the wheelset to follow the expected value. The designed fuzzy controller can reasonably allocate the speed of the left and right wheels in the wheelset, take into account the control of the wheelset translational speed, and improve the overall stability of the chassis motion.

(2) A MATLAB/Simulink ADAMS chassis joint simulation platform has been established, and the simulation results show that the wheelset steering angle control system designed in this paper is reasonable and feasible, and can meet the requirements of chassis turning and diagonal obstacle crossing during travel.

References

[1] Q. W. Wang, Zhao, Y. Q. Zhao, Deng, Y.J. Deng et al.，Optimal Coordinated Control of ARS and DYC for Four-wheel Steer and In-wheel Motor Driven Electric Vehicle with Unknown Tire Model[J]， IEEE Trans. Veh. Technol, 69 (10) (2020) 10809-10819.

[2] N. Zhang, J. Ni, J Hu, Robust H sub∞/sub state feedback control for handling stability of intelligent vehicles on a novel all-wheel independent steering mode[J]， IET Intelligent Transport Systems, 13(10) (2019) 1579-1589.

[3] F. Fahimi, Full drive-by-wire dynamic control for four-wheel-steer all-wheel-drive vehicles[J], VEHICLE SYSTEM DYNAMICS, 2013, 51 (3) (2013) 360-376.

[4] T. Xu, X. Liu, F. W. Wu, A Sliding Mode Control Scheme for Steering Flexibility and Stability in All-wheel-steering Multi-axle Vehicles[J], INTERNATIONAL JOURNAL OF CONTROL AUTOMATION AND SYSTEMS, 21 (6) (2023) 1926-1938.

[5] J. Wang, Q. Wang, (...)， C. Song, Independent wheel torque control of 4WD electric vehicle for differential drive assisted steering[J], MECHATRONICS, 21 (1) (2011) 63-76.

[6] J. Wang, R. G. Longoria, Coordinated and Reconfigurable Vehicle Dynamiics Control[J], IEEE Transactions on Control Systems Technology, 17 (3) (2009) 723-732

[7] J. Kim, M. El-Gindy, Z. El-Sayegh, Simulation and Validation of an 8 x 8 Scaled Electric Combat Vehicle[J], MACHINES, 12 (2) (2024).

[8] J. Ni, J. B. Hu, C. L. Xiang, An AWID and AWIS X-By-Wire UGV: Design and Hierarchical Chassis Dynamics Control[J], IEEE TRANSACTIONS ON INTELLIGENT TRANSPORTATION SYSTEMS, 20 (2) (2019) 654-666.

[9] M. Kuslits, D. Bestle, Modelling and control of a new differential steering concept[J], VEHICLE SYSTEM DYNAMICS, 57 (4) (2019)520-542.

[10] T. Chen, X. Xu, Y, Li, W. Wang, L. Chen, Speed-dependent coordinated control of differential and assisted steering for in-wheel motor driven electric vehicles [J], PROCEEDINGS OF THE INSTITUTION OF MECHANICAL ENGINEERS PART D-JOURNAL OF AUTOMOBILE ENGINEERING, 232 (9) (2018) 1206-1220.

[11] C. Wang, W. Zhao, Z. Luan, Q. Gao, K. Deng, Decoupling control of vehicle chassis system based on neural network inverse system [J], MECHANICAL SYSTEMS AND SIGNAL PROCESSING, 106 (2018) 176-197.

[12] Oftadeh. Reza, M. Mohammad, Reza. Aref, Ghabcheloo, Mattila Jouni, Mechatronic Design of a Four Wheel Steering Mobile Robot with Fault-Tolerant Odometry Feedback[J], IFAC Proceedings Volumes, 46 (5) (2013) 663-669.

[13] Yiran. Qiao, Xinbo. Chen, Zhen. Liu, Trajectory Tracking Coordinated Control of 4WID-4WIS Electric Vehicle Considering Energy Consumption Economy Based on Pose Sensors[J], Sensors, 23 (12) (2023).

[14] A.T. Nguyen, C. Sentouh, J. C. Popieul, Fuzzy steering control for autonomous vehicles under actuator saturation: Design and experiments[J], JOURNAL OF THE FRANKLIN INSTITUTE-ENGINEERING AND APPLIED MATHEMATICS, 355 (18) (2018) 9374-9395.

[15] S. Thanok, M. Parnichkun, Longitudinal control of an intelligent vehicle using particle swarm optimization based sliding mode control[J], ADVANCED ROBOTICS, 29 (8) (2015) 525-543.

[16] A.T. Nguyen, C. Sentouh, H. Zhang, J.C. Popieul, Fuzzy Static Output Feedback Control for Path Following of Autonomous Vehicles with Transient Performance Improvements, IEEE Trans. Intell. Transp. Syst. , (2019) 1–11.

[17] D. Lovarelli, Bacenetti, J. Bacenetti, Exhaust gases emissions from agricultural tractors: State of the art and future perspectives for machinery operators, Biosyst. Eng. , 186 (2019) 204–213.